JOURNAL OF GUIDANCE, CONTROL, AND DYNAMICS
Vol. 21, No. 1, January–February 1998

Optimization Procedure for Preliminary Design of Opposition-Class Mars Missions

Lorenzo Casalino,* Guido Colasurdo,† and Dario Pastrone‡
Politecnico di Torino, Turin 10129, Italy

A numerical procedure, based on the theory of optimal control, is developed and used to find the flight opportunities for a manned mission to Mars. High-thrust (impulsive) missions are considered; burns can occur either inside or outside the planets' spheres of influence. Venus flyby opportunities also are exploited, and time constraints are often present. The necessary conditions for optimality, derived to deal with such complex missions, constitute an extension of Lawden's primer vector theory. In particular, the optimal transfers that occur in a syzygistic period and that belong to the opposition class are analyzed, taking the eccentricity and inclination of the planetary orbits into account; adjustments produced by the addition of time constraints are discussed.

Introduction

THE next century probably will see a manned mission to Mars. Suitable round-trip trajectories are already known[1–3] and have been classified as the same Earth–Mars phase angle repeats after a synodic period of approximately 2.13 years. The most interesting missions for the early phase of human exploration of Mars use the unpowered flyby of the planet Venus to reduce propellant requirements and mission time lengths. The orbital periods of the three planets are to some extent commensurable, and relative angular positions repeat after a syzygistic period[4] of 6.4 years, which contains almost exactly three Earth–Mars and four Earth–Venus synodic periods. The planets, however, move on elliptic inclined orbits, and the same relative positions may occur only if the Earth, after an integer number of years, occupies the same position on its orbit, that is, every 5 syzygistic periods, which constitute a 32-year syzygistic cycle (if only the Earth–Mars relative position is concerned, a good repetition also is obtained after 7 and 8 synodic periods).

However, the planets' relative positions repeat only approximately, and a preliminary mission design cannot be avoided. The flight opportunities usually are found by using the two-body (sun–spacecraft) problem formulation. Parametric analyses with graphical aids[5] were widely used in the past for the simplest problems, but manned Mars missions need round-trip trajectories and short total duration; the problem is complicated by the presence of time constraints, midcourse impulses, and flybys. The number of unknown parameters increases, and the use of some automatic procedures, e.g., the new genetic algorithms,[6] is advisable. The authors propose an indirect optimization procedure, based on the theory of optimal control, for the preliminary analysis of interplanetary missions. The procedure is applied to find opportunities for a manned mission to Mars at the beginning of the next century. These opportunities are already known, and although the investigated period is no longer of practical interest for manned missions, the problem is quite complex and constitutes an adequate benchmark for the proposed procedure.

The indirect approach for the optimization of impulsive interplanetary trajectories using the matched-conic formulation was introduced by Glandorf.[7] At the moment, numerical codes,[8,9] based on the same approach, are available for the analysis of complex missions. A similar procedure is proposed here but the analysis is carried out in the heliocentric frame. This simpler procedure, which is adequate for preliminary analyses, minimizes the propellant consumption for rather complex interplanetary missions. For this purpose, if a favorable orientation of the parking orbits is assumed, the periapsis of the planetocentric hyperbolas must be fixed to the minimum allowable value and the optimal heliocentric trajectory is actually independent of the parking orbits around the planets. The mission therefore is composed of a succession of heliocentric ballistic arcs that join at planetary intercepts and midcourse impulses, where the spacecraft velocity is discontinuous. The theory of optimal control is applied to this impulsive problem but, in comparison to Lawden's primer vector theory[10] and subsequent applications,[11,12] the necessary conditions for optimality take the actual velocity impulse instead of the hyperbolic excess velocity into account; further conditions ensure the trajectory optimality in the presence of an unpowered, free-height Venus flyby. Time constraints can be imposed on the time length of the overall trajectory, the inbound and outbound legs, or the Mars stay. The necessary optimum conditions also are derived in the presence of these constraints. A better estimate of flight times may be required after the preliminary analysis; in some cases, a plane change between the parking orbit and the inbound or outbound hyperbola is needed. The optimization in the heliocentric frame becomes insufficient, and more powerful codes[8,9] should be used.

The optimal trajectories are obtained by numerically solving the boundary value problem (BVP), which arises from the indirect approach to the problem. The authors use a BVP solver that they developed[13] to match the analytical construction of the problem. The mission opportunities in the syzygistic period starting on June 20, 2000 (when Earth, Mars, and Venus are almost aligned with the sun), are analyzed. Opposition-class, high-thrust trajectories are considered, taking into account simple inbound or outbound legs (with only departure and arrival impulses), three-impulse legs (departure, midcourse, and arrival impulses), and flyby legs (a Venus flyby replaces the midcourse impulse).

Statement of the Problem

In the present approach the trajectory is considered to be composed of a succession of ballistic arcs that are separated by points where the spacecraft velocity undergoes jumps. The equations of motion of a spacecraft under the influence only of the sun's gravitational acceleration $\boldsymbol{g}(\boldsymbol{r})$ are

$$\dot{\boldsymbol{r}} = \boldsymbol{v} \tag{1}$$

$$\dot{\boldsymbol{v}} = \boldsymbol{g} \tag{2}$$

The Hamiltonian function is defined as

$$H = \boldsymbol{\lambda}_r^T \boldsymbol{v} + \boldsymbol{\lambda}_v^T \boldsymbol{g} \tag{3}$$

Presented as Paper 95-305 at the AAS/AIAA Astrodynamics Conference, Halifax, NS, Canada, Aug. 14–17, 1995; received Aug. 12, 1996; revision received July 1, 1997; accepted for publication July 7, 1997.

*Researcher, Dipartimento di Energetica, Corso Duca degli Abruzzi 24.
†Professor, Dipartimento di Energetica, Corso Duca degli Abruzzi 24. Member AIAA.
‡Researcher, Dipartimento di Energetica, Corso Duca degli Abruzzi 24. Member AIAA.

whereas the adjoint equations for the problem are

$$\dot{\boldsymbol{\lambda}}_r^T = -\frac{\partial H}{\partial \boldsymbol{r}} = -\boldsymbol{\lambda}_v^T G \tag{4}$$

$$\dot{\boldsymbol{\lambda}}_v^T = -\frac{\partial H}{\partial \boldsymbol{v}} = -\boldsymbol{\lambda}_r^T \tag{5}$$

where $G(\boldsymbol{r})$ is the gravity-gradient matrix. The procedure searches for the trajectory that achieves the rendezvous with the relevant planets while minimizing the characteristic velocity, which is the performance index

$$\varphi = \Delta V = \sum_i \Delta v_i \tag{6}$$

The characteristic velocity ΔV is the arithmetic sum of the velocity changes that are performed by expending the propellant. The definition of Δv_i is trivial for a midcourse impulse but, if the spacecraft leaves or reaches a planetocentric orbit, one obtains

$$\Delta v_i = \sqrt{(\boldsymbol{v}_i - \boldsymbol{v}_P)^2 + v_e^2} - v_a \tag{7}$$

where $\boldsymbol{v}_P(t)$ is the velocity vector of the planet around the sun and v_e and v_a are the magnitudes of the planet-relative escape and actual velocities, respectively, at the periapsis of the planetocentric trajectory. Note that a different performance index φ^* often is minimized in similar analyses; this index uses the hyperbolic excess velocity, i.e., $v_e = v_a = 0$ in Eq. (7), instead of the actual velocity impulse at the hyperbola periapsis.

Necessary Transversality Conditions

The authors' approach to the optimization of spacecraft trajectories preliminarily assumes the switching structure. The trajectory, i.e., the integration interval, is split into succeeding subintervals in which simple control strategies are assumed. The present problem also has been posed in a rather peculiar form: no control rules the ballistic arcs, whereas jumps in the state variables occur at every interior point. According to Bryson and Ho,[14] quite general expressions for the necessary transversality conditions are

$$\left[H_{j_-} + \frac{\partial \varphi}{\partial t_{j_-}} + \boldsymbol{\mu}^T \frac{\partial \boldsymbol{\chi}}{\partial t_{j_-}}\right] \delta t_{j_-} = 0 \tag{8}$$

$$\left[-H_{j_+} + \frac{\partial \varphi}{\partial t_{j_+}} + \boldsymbol{\mu}^T \frac{\partial \boldsymbol{\chi}}{\partial t_{j_+}}\right] \delta t_{j_+} = 0 \tag{9}$$

$$\left[-\boldsymbol{\lambda}_{j_-}^T + \frac{\partial \varphi}{\partial \boldsymbol{x}_{j_-}} + \boldsymbol{\mu}^T \frac{\partial \boldsymbol{\chi}}{\partial \boldsymbol{x}_{j_-}}\right] \delta \boldsymbol{x}_{j_-} = 0 \tag{10}$$

$$\left[\boldsymbol{\lambda}_{j_+}^T + \frac{\partial \varphi}{\partial \boldsymbol{x}_{j_+}} + \boldsymbol{\mu}^T \frac{\partial \boldsymbol{\chi}}{\partial \boldsymbol{x}_{j_+}}\right] \delta \boldsymbol{x}_{j_+} = 0 \tag{11}$$

where φ is the function that must be minimized, $\boldsymbol{\chi}$ is the vector of the constraints, and $\boldsymbol{\mu}$ collects the constant multipliers associated with each constraint. These constants are distinguished by subscripts that refer to the related constraints and are eliminated when deriving the necessary optimum conditions. Subscripts $-$ and $+$ denote the value just before and after the jth point, respectively. Equations (8) and (10) are meaningless at the initial point, whereas Eqs. (9) and (11) are meaningless at the final point.

A systematic application of Eqs. (8–11) is sufficient to obtain suitable boundary conditions for the numerical optimization of a specific mission once its switching structure is assumed. As an example, the conditions for an optimal opposition-class trajectory are given. The spacecraft leaves Earth (subscript 0) and reaches Mars (subscript 2_-) using a midcourse burn (subscript 1). After a short stay, the spacecraft returns from Mars (subscript 2_+) to Earth (subscript 4), but the homebound flight is made more efficient by means of a swingby at Venus (subscript 3). Different mission scenarios would affect only the number and order of the discontinuity points.

Earth Departure and Arrival

At the initial point of the trajectory, the only effective constraint is $\boldsymbol{r}_0 = \boldsymbol{r}_\oplus(t_0)$. By applying Eq. (11), one obtains

$$\boldsymbol{\lambda}_{r0} = \boldsymbol{\mu}_0 \tag{12}$$

$$\boldsymbol{\lambda}_{v0} = \frac{\boldsymbol{v}_0 - \boldsymbol{v}_{\oplus 0}}{\sqrt{(\boldsymbol{v}_0 - \boldsymbol{v}_{\oplus 0})^2 + v_{e0}^2}} \tag{13}$$

Whereas the position adjoint vector is free, the velocity adjoint vector or primer vector[10] is parallel to the hyperbolic excess velocity $\boldsymbol{v}_\infty = \boldsymbol{v}_0 - \boldsymbol{v}_{\oplus 0}$. Equation (13) also prescribes the primer magnitude, which depends only on the hyperbolic excess velocity and the periapsis of the planetocentric trajectory. The actual apoapsis of the parking orbit, which is related to v_a, determines the characteristic velocity through Eq. (7) but does not affect the boundary conditions and therefore the geometry of the heliocentric trajectory. This is not surprising because it is well known that, for instance, a re-entering spacecraft can reach the final Earth orbit with the same propellant expenditure when either a single perigee maneuver or subsequent perigee impulsive burns are executed.

If the departure time is left open, Eq. (9) provides

$$H_0 - \frac{(\boldsymbol{v}_0 - \boldsymbol{v}_{\oplus 0})^T}{\sqrt{(\boldsymbol{v}_0 - \boldsymbol{v}_{\oplus 0})^2 + v_{e0}^2}} \dot{\boldsymbol{v}}_{\oplus 0} - \boldsymbol{\mu}_0^T \boldsymbol{v}_{\oplus 0} = 0 \tag{14}$$

which, by using Eqs. (3), (12), and (13) and considering that the Earth also obeys Eq. (2), reduces to

$$\boldsymbol{\lambda}_{r0}^T(\boldsymbol{v}_0 - \boldsymbol{v}_{\oplus 0}) = 0 \tag{15}$$

By taking again Eq. (13) into account, Eq. (15) is found to be equivalent to

$$\boldsymbol{\lambda}_{r0}^T \boldsymbol{\lambda}_{v0} = \dot{\boldsymbol{\lambda}}_{v0}^T \boldsymbol{\lambda}_{v0} = \dot{\lambda}_{v0} \lambda_{v0} = 0 \tag{16}$$

Equation (16) states the stationarity of the primer magnitude ($\dot{\lambda}_{v0} = 0$) because λ_{v0} cannot be zero.

The application of Eqs. (8) and (10) at Earth arrival produces similar results. For instance,

$$\boldsymbol{\lambda}_{v4} = \frac{\boldsymbol{v}_{\oplus 4} - \boldsymbol{v}_4}{\sqrt{(\boldsymbol{v}_4 - \boldsymbol{v}_{\oplus 4})^2 + v_{e4}^2}} \tag{17}$$

which corresponds to Eq. (13) and reminds one that the primer vector points in the same direction as the change of the heliocentric velocity.

Midcourse Impulse

The contribution of midcourse burns to characteristic velocity is related only to the change of the sun-relative velocity

$$\Delta v_1 = \sqrt{\left(\boldsymbol{v}_{1_+} - \boldsymbol{v}_{1_-}\right)^2} \tag{18}$$

As the position and time are open, constraints $\boldsymbol{r}_{1_+} = \boldsymbol{r}_{1_-}$ and $t_{1_+} = t_{1_-}$ are taken into account. By using Eqs. (10) and (11), one easily deduces $\boldsymbol{\lambda}_{r1_+} = \boldsymbol{\lambda}_{r1_-}$ and

$$\boldsymbol{\lambda}_{v1_+} = \boldsymbol{\lambda}_{v1_-} = \frac{\boldsymbol{v}_{1_+} - \boldsymbol{v}_{1_-}}{\sqrt{\left(\boldsymbol{v}_{1_+} - \boldsymbol{v}_{1_-}\right)^2}} \tag{19}$$

The continuity of the Hamiltonian also is found by means of Eqs. (8) and (9). According to Eq. (3), one obtains $\boldsymbol{\lambda}_{r1}^T(\boldsymbol{v}_{1_+} - \boldsymbol{v}_{1_-}) = 0$, which again implies the stationarity of the primer magnitude.

One could minimize a multiple of the characteristic velocity by adding an arbitrary coefficient into Eq. (6). Such a coefficient, which would scale the adjoint vector magnitudes up or down, has intentionally been omitted, and the primer magnitude is therefore unity when the spacecraft uses its engine in the gravitational field of the main attractive body, according to the prevailing literature. In the present problem the thrust often is used inside the sphere of influence of a planet. In these circumstances, the primer magnitude must be reduced by an amount that depends on the hyperbolic excess velocity and periapsis of the planetocentric trajectory.

Mars Arrival and Departure

If the time length of the Mars stay is left open, the same boundary conditions apply as for Earth at both arrival and departure. The corresponding minimum-fuel trajectories, which belong to the conjunction class, are characterized by the long Mars stay times that are required to wait for adequate Mars–Earth phasing. To reduce the overall durations, a constraint on the stay time $t_{2+} - t_{2-} = \tau_2$ therefore must be added to the position constraints $\boldsymbol{r}_{2-} = \boldsymbol{r}_{\male}(t_{2-})$ and $\boldsymbol{r}_{2+} = \boldsymbol{r}_{\male}(t_{2+})$. The presence of the time constraint does not modify the application of Eqs. (10) and (11), which provides $\boldsymbol{\lambda}_{r2-} = -\boldsymbol{\mu}_{21}$, $\boldsymbol{\lambda}_{r2+} = \boldsymbol{\mu}_{22}$, and

$$\boldsymbol{\lambda}_{v2-} = \frac{\boldsymbol{v}_{\male -} - \boldsymbol{v}_{2-}}{\sqrt{\left(\boldsymbol{v}_{2-} - \boldsymbol{v}_{\male -}\right)^2 + v_{e2-}^2}} \tag{20}$$

$$\boldsymbol{\lambda}_{v2+} = \frac{\boldsymbol{v}_{2+} - \boldsymbol{v}_{\male +}}{\sqrt{\left(\boldsymbol{v}_{2+} - \boldsymbol{v}_{\male +}\right)^2 + v_{e2+}^2}} \tag{21}$$

By means of Eqs. (8) and (9), one obtains, respectively,

$$-H_{2-} + \frac{\left(\boldsymbol{v}_{\male -} - \boldsymbol{v}_{2-}\right)^T}{\sqrt{\left(\boldsymbol{v}_{2-} - \boldsymbol{v}_{\male -}\right)^2 + v_{e2-}^2}} \dot{\boldsymbol{v}}_{\male -} - \boldsymbol{\mu}_{21}^T \boldsymbol{v}_{\male -} - \mu_{23} = 0 \tag{22}$$

$$H_{2+} - \frac{\left(\boldsymbol{v}_{2+} - \boldsymbol{v}_{\male +}\right)^T}{\sqrt{\left(\boldsymbol{v}_{2+} - \boldsymbol{v}_{\male +}\right)^2 + v_{e2+}^2}} \dot{\boldsymbol{v}}_{\male +} - \boldsymbol{\mu}_{22}^T \boldsymbol{v}_{\male +} + \mu_{23} = 0 \tag{23}$$

which are combined to provide

$$\boldsymbol{\lambda}_{r2+}^T \left(\boldsymbol{v}_{2+} - \boldsymbol{v}_{\male +}\right) + \boldsymbol{\lambda}_{r2-}^T \left(\boldsymbol{v}_{\male -} - \boldsymbol{v}_{2-}\right) = 0 \tag{24}$$

The conditions that prescribed the stationarity of the primer magnitude at the time-open Mars arrival and departure have been replaced by the time constraint and Eq. (24), which is actually a relation between the time derivatives of the primer magnitude, which are proportional to the corresponding hyperbolic excess velocities but have the opposite sign.

Unpowered Venus Flyby

The intercept of Venus introduces the constraints $\boldsymbol{r}_{3+} = \boldsymbol{r}_{3-} = \boldsymbol{r}_{\female}(t_{3-})$ and $t_{3+} = t_{3-}$. Moreover, the magnitude of the planet-relative velocity is preserved:

$$\left(\boldsymbol{v}_{3+} - \boldsymbol{v}_{\female}\right)^2 = \left(\boldsymbol{v}_{3-} - \boldsymbol{v}_{\female}\right)^2 \tag{25}$$

By applying Eqs. (10) and (11), one obtains

$$\boldsymbol{\lambda}_{r3+} - \boldsymbol{\lambda}_{r3-} = \boldsymbol{\mu}_{32} \tag{26}$$

(the position adjoint vector is discontinuous) and

$$\boldsymbol{\lambda}_{v3-} = 2\mu_{33}\left(\boldsymbol{v}_{3-} - \boldsymbol{v}_{\female}\right) \tag{27}$$

$$\boldsymbol{\lambda}_{v3+} = 2\mu_{33}\left(\boldsymbol{v}_{3+} - \boldsymbol{v}_{\female}\right) \tag{28}$$

The primer vector is therefore parallel to the hyperbolic excess velocity, and its magnitude is continuous. The necessary transversality conditions that concern the Hamiltonian provide

$$H_{3+} - H_{3-} - \boldsymbol{\mu}_{32}^T \boldsymbol{v}_{\female} - 2\mu_{33}\left[\left(\boldsymbol{v}_{3+} - \boldsymbol{v}_{\female}\right)^T - \left(\boldsymbol{v}_{3-} - \boldsymbol{v}_{\female}\right)^T\right]\dot{\boldsymbol{v}}_{\female} = 0 \tag{29}$$

which is easily reduced to the form

$$\boldsymbol{\lambda}_{r3+}^T \left(\boldsymbol{v}_{3+} - \boldsymbol{v}_{\female}\right) - \boldsymbol{\lambda}_{r3-}^T \left(\boldsymbol{v}_{3-} - \boldsymbol{v}_{\female}\right) = 0 \tag{30}$$

Equation (30) essentially states that the time derivative of the primer magnitude is also continuous.

In some problems, the optimal solution could imply an approach that is too close to the planet; a further constraint concerning the minimum height should be added, and Eqs. (27) and (28) would be modified.[15] This constraint actually is not required for the missions that are presented.

Numerical Solution

The procedure for the numerical solution of the differential problem first assumes the mission structure, or switching structure, that is, a suitable succession of planetary arrivals, departures, flybys, and midcourse impulses.[13] By supporting the differential equations (1), (2), (4), and (5) with the relevant boundary conditions, a BVP is posed and numerically solved. The solution therefore is inspected to decide whether the switching structure must be modified. A midcourse impulse is added, for instance, where the primer magnitude exceeds unity; a similar procedure also is followed by classical indirect methods for time-fixed impulsive maneuvers.[11,12]

Indirect techniques for impulsive transfers often use some type of gradient method in the numerical solution. The authors instead have extended a technique that is typical of finite-thrust transfers to impulsive maneuvers. A shooting procedure that exploits the numerical integration of the sensitivity equations is used.[13] The numerical efficiency is improved by a particular treatment of the interior points that allows the contemporary optimization of the whole trajectory instead of separately matching optimized arcs.

The theory of optimal control provides conditions that are necessary but not sufficient for the global optimality of the numerical solution. In the most common applications, for instance, Earth satellite maneuvers, the main difficulty is that of supplying a tentative solution that is close enough to guarantee convergence to the optimal solution. When interplanetary missions are analyzed, the investigated period is, of necessity, limited and comparable to mission time lengths; the global optimum usually is seen as the least expensive occasion among several local minima or mission opportunities that are the true objective of the procedure. Their number grows with the mission complexity, and the main difficulty becomes that of being sure that interesting opportunities have not been neglected.

Results

The present analysis is more directed to the qualitative and theoretical aspects of the problem than to the actual design of a mission. The sun's gravitational field therefore is accounted for by means of an inverse square law, and the planet orbits thus are described by the six constant orbital elements.

The procedure is used to find the mission opportunities that correspond to a local minimum of the characteristic velocity; the influence of the flight time on the mission cost is neglected. The spacecraft leaves a 500-km-altitude circular Earth orbit and reaches a 1-sol Mars orbit with a 3800-km periapsis radius; the same parking orbits are assumed for the return leg. Ascents to a parking orbit, as well as descents from it, are not considered; a favorable orientation of the parking orbits is always assumed.

Opposition-Class Trajectories

This paper does not deal with conjunction-class trajectories, which constitute the simplest and least expensive mission concept. These missions wait on Mars for a favorable Earth position, and the time lengths of the Mars stay and whole mission may be excessive for the first phase of the Mars exploration. However, the present methodology also has been applied to these missions.[16,17]

The Mars stay of the opposition-class trajectories is instead limited to 30–60 days; a corresponding constraint must explicitly be imposed because a shorter stay would reduce the mission characteristic velocity. Round-trip flight times are brief with respect to conjunction-class missions, whereas ΔV requirements are up to 60% higher. Because the planets are not in a favorable position in either leg, a midcourse impulse is advisable: The spacecraft needs to travel faster and approaches the sun at 0.6–0.7 AU, where an impulse corrects the trajectory in order to reach the target planet. These mission opportunities depend only on the Earth–Mars phase angle; three trajectories (one for each synodic period) with the midcourse impulse during the outbound leg (O1, O2, O3) and three during the inbound leg (I1, I2, I3) are found for a 60-day Mars stay in the examined syzygistic period; their characteristics are presented in Table 1, and a synoptic view is provided in Fig. 1.

Significant differences in ΔV are shown by the 2000 and 2005 missions (O1 and I3). The latter, which also has the longest flight

Table 1 Opposition-class trajectories

Mission	⊕ Launch date (Δv, km/s)	Midcourse date (Δv, km/s)	♂ Arrival date (Δv, km/s)	♂ Departure date (Δv, km/s)	Midcourse date (Δv, km/s)	⊕ Return date (Δv, km/s)	Δt, days (ΔV, km/s)
O1	03/26/00	08/18/00	02/18/01	04/19/01	——	11/09/01	593.0
	(4.228)	(3.984)	(3.423)	(1.567)	——	(4.641)	(17.844)
I1	03/23/01	——	09/20/01	11/19/01	04/30/02	10/20/02	576.5
	(3.556)	——	(1.772)	(3.213)	(3.069)	(3.782)	(15.392)
O2	05/13/02	10/16/02	04/14/03	06/13/03	——	11/26/03	561.6
	(3.935)	(3.263)	(3.401)	(1.565)	——	(3.635)	(15.799)
I2	05/15/03	——	11/05/03	01/04/04	07/04/04	12/02/04	566.9
	(3.724)	——	(1.548)	(3.369)	(3.299)	(3.901)	(15.841)
O3	07/04/04	12/30/04	06/08/05	07/08/05	——	04/15/06	649.4
	(3.741)	(3.137)	(3.108)	(1.690)	——	(3.955)	(15.631)
I3	02/13/05	——	10/04/05	12/03/05	06/30/06	12/15/06	670.3
	(6.497)	——	(2.265)	(2.421)	(3.260)	(3.485)	(17.928)
I3a	10/19/04	03/04/05	08/17/05	10/16/05	05/23/06	11/20/06	761.8
	(3.715)	(2.392)	(2.615)	(2.013)	(2.807)	(3.303)	(16.846)
I1s	04/10/01	——	09/07/01	10/07/01	03/18/02	06/24/02	440.0
	(3.759)	——	(2.303)	(3.492)	(1.702)	(4.738)	(15.994)
I1t	04/02/01	——	09/11/01	11/10/01	04/25/02	08/15/02	500.0
	(3.624)	——	(2.059)	(3.951)	(2.151)	(4.382)	(16.168)

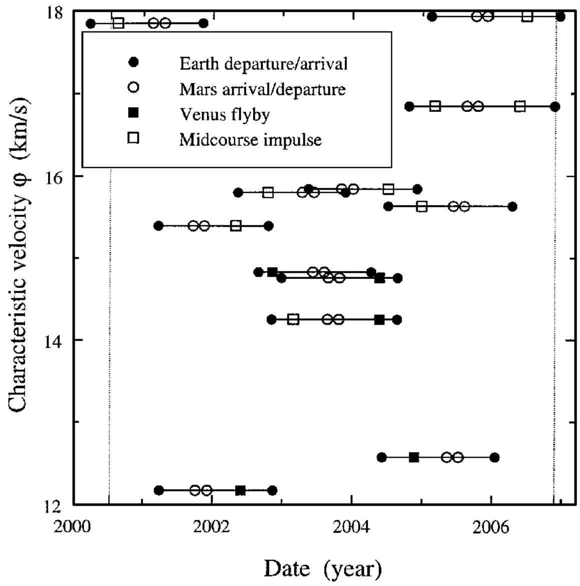

Fig. 1 Synoptic view of mission opportunities.

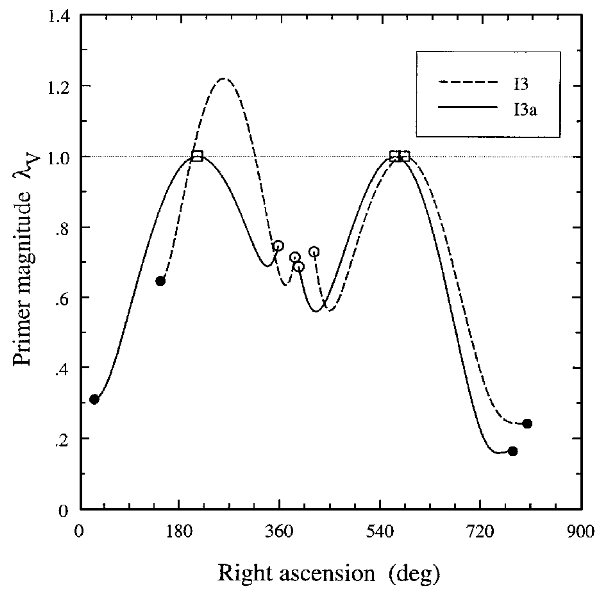

Fig. 2 Primer magnitude during opposition-class missions (I3 and I3a in Table 1) (see legend to Fig. 1).

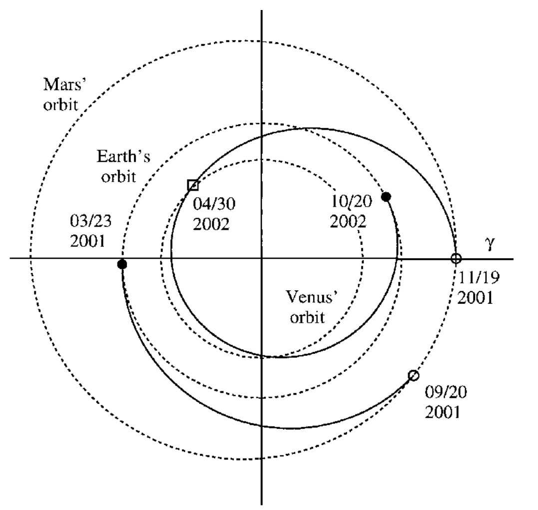

Fig. 3 Minimum φ trajectory (φ = 15.392; φ^* = 20.012) (see legend to Fig. 1).

time, is particular, i.e., nonoptimal; the primer magnitude exceeds unity during the outbound leg (dotted line in Fig. 2), and Pontryagin's principle is not satisfied. The switching structure is modified by adding an impulse, and the corresponding solution (I3a in Table 1) fulfills the necessary optimum conditions (solid line in Fig. 2) but still corresponds to a rather expensive local minimum. Notice that the 2005 trajectory, without the outbound midcourse impulse, becomes optimal if the stay time is reduced to 30 days.

The projection of the I1 trajectory onto the ecliptic plane is shown in Fig. 3. A similar and contemporary mission is presented in Fig. 4, but it minimizes the cost index φ^*, which has been constructed by assuming $v_e = v_a = 0$ in Eq. (7), i.e., by considering the hyperbolic excess velocity instead of the actual velocity impulse. In this case, $\lambda_V = 1$ is imposed not only at the midcourse impulses (an additional burn is required during the outbound leg) but also in correspondence to Earth and Mars (Fig. 5).

The flight time can be reduced by imposing a constraint on the total time length of the mission (while the constraint on the Mars stay is maintained). Two trajectories, derived from the I1 mission, are added to Table 1. The 440-day or sprint mission (I1s), with the Mars stay limited to 30 days, presents a time length that is comparable to current experience for flight crews; the 500-day mission (I1t), with a 60-day Mars stay, is a compromise between sprint and opposition-class trajectories. The characteristic velocities are only 4–5% higher.

Flyby Trajectories

The midcourse impulse, which occurs near Venus' orbit (see Fig. 3), in favorable circumstances can be replaced by a flyby. The

Table 2 Venus flyby trajectories

Mission	⊕ Launch date (Δv, km/s)	♀ Flyby date	Midcourse date (Δv, km/s)	♂ Arrival date (Δv, km/s)	♂ Departure date (Δv, km/s)	♀ Flyby date	⊕ Return date (Δv, km/s)	Δt, days (ΔV, km/s)
FI3	03/29/01	——	——	10/06/01	12/05/01	05/30/02	11/16/02	596.8
	(3.587)	——	——	(1.467)	(3.108)	——	(4.011)	(12.173)
FO5	08/28/02	11/10/02	——	06/10/03	08/09/03	——	04/08/04	589.7
	(4.163)	——	——	(3.524)	(2.137)	——	(5.004)	(14.827)
FI5	12/27/02	——	——	08/29/03	10/28/03	05/23/04	08/25/04	606.5
	(5.293)	——	——	(2.281)	(3.327)	——	(3.857)	(14.758)
FI5a	11/07/02	——	02/26/03	08/24/03	10/23/03	05/22/04	08/23/04	654.7
	(3.869)	——	(1.498)	(2.073)	(3.091)	——	(3.719)	(14.250)
FO3	06/06/04	11/20/04	——	05/12/05	07/11/05	——	01/18/06	590.6
	(4.099)	——	——	(3.263)	(1.559)	——	(3.654)	(12.576)

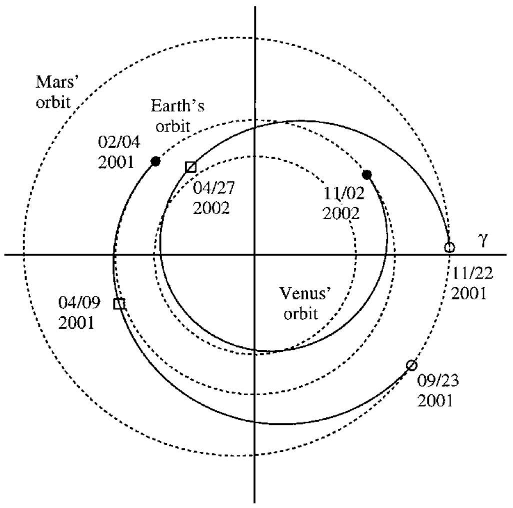

Fig. 4 Minimum φ^* trajectory (φ = 17.034; φ^* = 19.720) (see legend to Fig. 1).

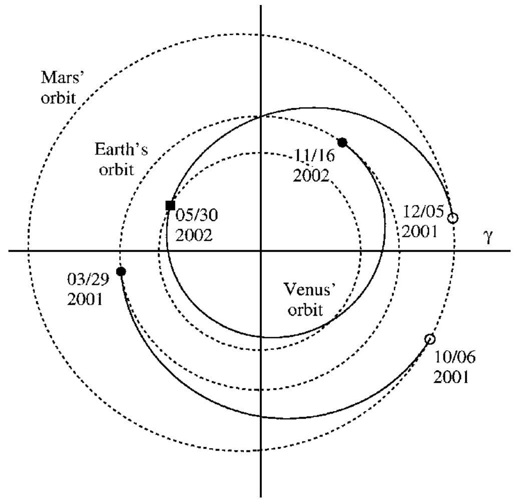

Fig. 6 Venus-flyby trajectory (FI3 in Table 2) (see legend to Fig. 1).

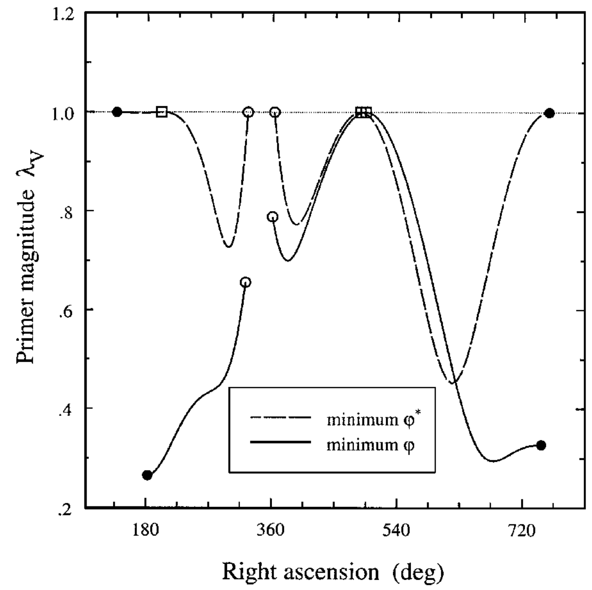

Fig. 5 Primer history for missions shown in Figs. 3 and 4 (see legend to Fig. 1).

spacecraft is sent toward Venus to obtain a free velocity change that reshapes the trajectory and provides a tangential approach to Mars' or Earth's heliocentric orbit. Table 2 provides launch dates, interplanetary flight times, and ΔV requirements for the missions that exploit the Venus flyby. A syzygistic period contains seven Mars–Venus synodic periods, and the same phase angle between Mars and Venus repeats seven times. Unfortunately, the Earth angular position is different and a quite favorable trajectory from Venus to Earth is only possible once (type-3 mission, according to Gillespie and Ross[4]). After two further Mars–Venus synodic periods, a less interesting opportunity (type-5 mission) occurs. Each trajectory that uses the swingby in the inbound leg (FI3, FI5) has a quite similar trajectory (FO3, FO5) traveled in the opposite direction. Type-3 trajectories closely correspond to the I1 and O3 opposition-class trajectories, but the Venus flyby has replaced the midcourse impulse and strongly reduced the characteristic velocity (see Fig. 1). The FI3 mission is shown in Fig. 6 (a solid square indicates the flyby).

The planets' angular positions exert more influence on the characteristic velocity than Mars' and Venus' orbital inclinations, which are rather low. Hence, simple legs span more than 90 deg, and the transfer arc inclination is higher than the declination of the intercept point and may be higher than Mars' orbital inclination. Three-impulse and flyby legs behave similarly to simple legs; the midcourse impulse (or the flyby) has the primary task of phasing the spacecraft to the target planet but, thanks to the plane change during the transfer arc, has the secondary effect of keeping the plane rotations lower at departure and arrival. As an example, Fig. 7 shows the FI3 mission in the right ascension–declination plane.

The primer magnitude is larger than unity in the outbound leg of the FI5 trajectory. A midcourse impulse is added to fulfill Pontryagin's principle; the new trajectory (FI5a) is described in Table 2 and shown in Figs. 8 and 9. Notice that the 3% lower ΔV might not compensate for the disadvantages connected to the 8% higher flight time. The profile of the primer magnitude and its time derivative are shown in Fig. 10 for the same case. The mission closely corresponds to the sample case used to derive the necessary optimum conditions. Therefore, Fig. 10 provides a comprehensive summary of these conditions.

Other local minima can be found but are not given in Table 2 because their characteristic velocities and/or flight times are larger. Because the absolute positions of the planets are different in the following syzygistic periods, these opportunities might become interesting and should be assumed as tentative solutions for analyses

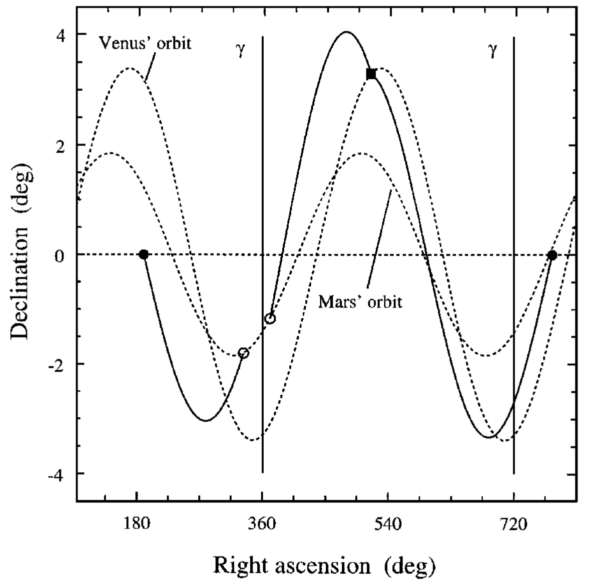

Fig. 7 Venus-flyby trajectory (FI3 in Table 2) in right ascension–declination plane (see legend to Fig. 1).

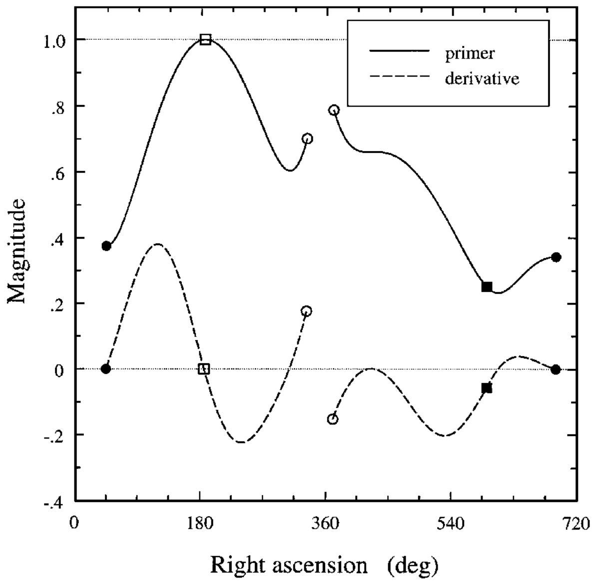

Fig. 10 Primer magnitude and time derivative during FI5a mission (see legend to Fig. 1).

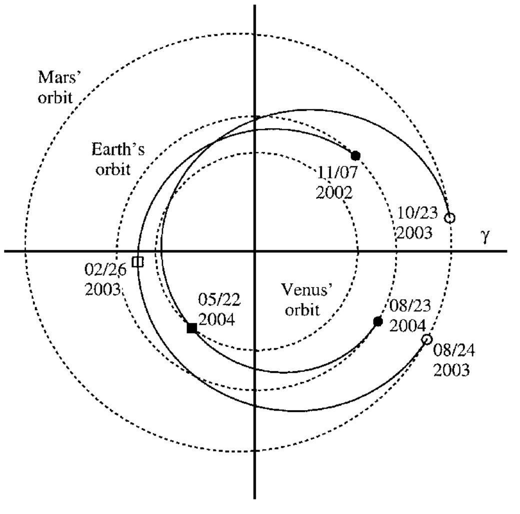

Fig. 8 Venus-flyby trajectory with additional impulse (FI5a in Table 2) (see legend to Fig. 1).

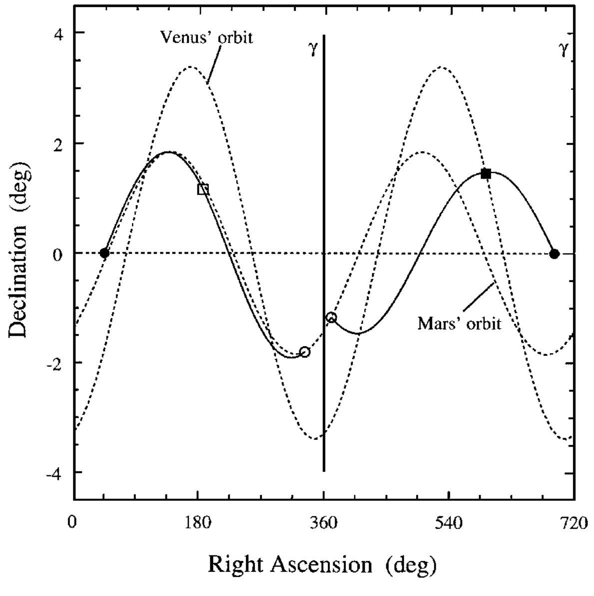

Fig. 9 Venus-flyby trajectory with additional impulse (FI5a in Table 2) (see legend to Fig. 1).

concerning other periods.[17] One should remark that the convergence of the procedure is easy when the same initial solution is assumed but times and phase angles are increased by a syzygistic period (and it is very easy in the case of a complete syzygistic cycle).

Conclusions

The authors present an indirect optimization method for the preliminary analysis of interplanetary missions based on two-body-problem equations in the heliocentric reference frame. The method, which is applicable to complex missions with several planetary rendezvous or flybys, is an extension of classical indirect methods for the optimization of simple orbital transfers. New necessary conditions for the primer vector and its time derivative have been obtained to optimize this kind of mission.

A few examples concerning the flight opportunities for a manned Mars mission have verified the theoretical achievements. The procedure attains a solution that is strongly related or close to the tentative solution. This characteristic makes the treatment of problems presenting many solutions that satisfy the optimum necessary conditions quite delicate. On the other hand, it permits one to find several mission opportunities in the same syzygistic period even though it is difficult to be sure that all opportunities have been found. If the analysis has to be extended to other periods, recurrences in the relative motion of the relevant planets permit the use of previous solutions as tentative solutions for the subsequent periods.

The accuracy and speed of the numerical procedure, i.e., of the BVP solver, have been proved for this class of impulsive problems, but numerical tests have confirmed that convergence is more difficult for impulsive maneuvers than finite-thrust problems. However, it would be useful and not difficult, at least for impulsive problems, to provide the procedure with a preliminary phase that gives an automatic guess at the adjoints and other unknown parameters.

Acknowledgment

This research was supported by the Ministero dell'Università e della Ricerca Scientifica e Tecnologica.

References

[1]Hoffman, S. J., McAdams, J. V., and Niehoff, J. C., "Round Trip Trajectory Options for Human Exploration of Mars," *Advances in the Astronautical Sciences*, Vol. 69, Univelt, San Diego, CA, 1989, pp. 663–679.

[2]Soldner, J. K., "Round-Trip Mars Trajectories: New Variations on Classic Mission Profiles," *Proceedings of the AIAA/AAS Astrodynamics Conference*, AIAA, Washington, DC, 1990, pp. 497–505 (AIAA Paper 90-2932).

[3]Walberg, G., "How Shall We Go to Mars? A Review of Mission Scenarios," *Journal of Spacecraft and Rockets*, Vol. 30, No. 2, 1993, pp. 129–139.

[4]Gillespie, R. W., and Ross, S., "Venus-Swingby Mission Mode and Its Role in the Manned Exploration of Mars," *Journal of Spacecraft and Rockets*, Vol. 4, No. 2, 1967, pp. 170–175.

[5]Lee, V. A., and Wilson, S. W., Jr., "A Survey of Ballistic Mars-Mission Profiles," *Journal of Spacecraft and Rockets*, Vol. 4, No. 2, 1967, pp. 129–142.

[6]Gage, P. J., Braun, R. D., and Kroo, I. M., "Interplanetary Trajectory Optimization Using a Genetic Algorithm," *Journal of the Astronautical Sciences*, Vol. 43, No. 1, 1995, pp. 59–75.

[7]Glandorf, D. R., "Primer Vector Theory for Matched-Conic Trajectories," *AIAA Journal*, Vol. 8, No. 1, 1970, pp. 155, 156.

[8]Friedlander, A., "(MULIMP) Multi-Impulse Trajectory and Mass Optimization Program," Science Applications, Inc., Rept. SAI-120-383-14, San Diego, CA, April 1974.

[9]Sauer, C. G., "MIDAS—Mission Design and Analysis Software for the Optimization of Ballistic Interplanetary Trajectories," *Journal of the Astronautical Sciences*, Vol. 37, No. 3, 1989, pp. 251–259.

[10]Lawden, D. F., *Optimal Trajectories for Space Navigation*, Butterworths, London, 1963, pp. 54–68.

[11]Lion, P. M., and Handelsman, M., "The Primer Vector on Fixed-Time Impulsive Trajectories," *AIAA Journal*, Vol. 6, No. 1, 1968, pp. 127–132.

[12]Prussing, J. E., and Chiu, J.-H., "Optimal Multiple-Impulse Time-Fixed Rendezvous Between Circular Orbits," *Journal of Guidance, Control, and Dynamics*, Vol. 9, No. 1, 1986, pp. 17–22.

[13]Colasurdo, G., and Pastrone, D., "Indirect Optimization Method for Impulsive Transfer," *Proceedings of the AIAA/AAS Astrodynamics Conference*, AIAA, Washington, DC, 1994, pp. 441–448 (AIAA Paper 94-3762).

[14]Bryson, A. E., and Ho, Y. C., *Applied Optimal Control*, Hemisphere, Washington, DC, 1975, p. 125.

[15]Pastrone, D., "Traiettorie Ottimali con Flyby," *Atti del XIII Congresso Nazionale AIDAA* (Rome, Italy), AIDAA, Rome, Italy, 1995, pp. 1115–1124.

[16]Casalino, L., Colasurdo, G., and Pastrone, D., "Optimal Three-Dimensional Trajectories for Manned Mars Missions," *Proceedings of the AIAA/AAS Astrodynamic Conference*, AIAA, Reston, VA, 1996, pp. 377–384 (AIAA Paper 96-3612).

[17]Casalino, L., Colasurdo, G., and Pastrone, D., "Mission Opportunities for Human Exploration of Mars," Second Italian Meeting on Celestial Mechanics, L'Aquila, Italy, April 1997; also *Planetary and Space Sciences* (to be published).